Electronic Supplementary Information(ESI)

Polybutene-1 tube with in-situ microfibering polystyrene via helical convergent flow: an economical pathway to continuously fabricate biaxially reinforced polyolefin tubes for medical application

Wei Liu, Min Nie*, Qi Wang

Address: State Key Laboratory of Polymer Materials Engineering, Polymer Research Institute of Sichuan University, Chengdu 610065, China

Email: poly.nie@gmail.com

Fax: +86-28-85405133

Tel: +86-28-85405133

Sample preparation

The raw materials used in this study were isotactic polybutene-1(PB-1) and polystyrene (PS). The PS (666H), which was used as microfibrillar candidates, was a general purpose polystyrene supplied in pellets by Styron with a melt flow index (MFI) of 8.0g/10min(200℃/5kg). The PB-1 matrix was P5250, a commercial products of Mitsui Chemicals Co. Ltd used for tubing extrusion, and its MFI was 0.4g/10min(190℃/2.16kg).

The granules of PB-1 and PS were pre-mixed in a weight ratio of 90/10 and then extruded into tubes by adopting a self designed apparatus shown as Figure 1.

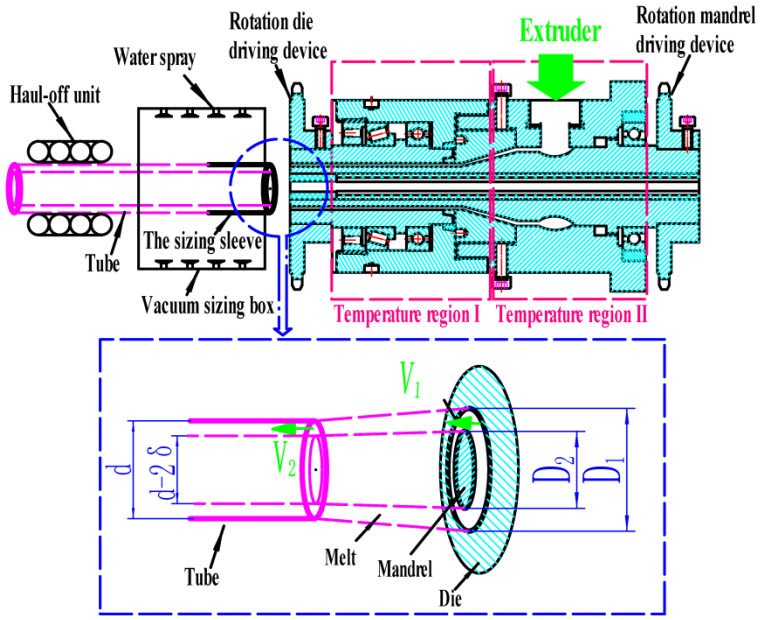

Figure 1. Schematic diagram of self-designed apparatus

By applying vacuum sizing sleeve with different dimensions and manipulating the ratio of extrusion/extraction rates, we can introduce a extensional convergent flow to the off-die melt with different convergent flow ratio (CFR), which was defied as the ratio of melt flow velocity after and before convergence and could be calculated from equation(1):

$$\phi = \frac{V_2}{V_1} = \frac{D_1^2 - D_2^2}{(2d\delta - \delta^2) \times \nabla} \qquad (1)$$

Where V_2 and V_1 were the melt flow rate in the sizing sleeve and the die respectively, D_1/D_2 were the external/internal diameters of the die, and d and δ were the external diameter and thickness of the produced tubes (as shown in Figure 1). The correction factor ∇, which is only related to the volume contraction of the melt during cooling, can be calculated according to the equation (2):

$$\nabla = \frac{[\rho_{amorph}(1 - X_c) + \rho_{crystal} X_c]\omega_{PB-1} + \rho_{PS} \times \omega_{PS}}{\rho_{amorph} \times \omega_{PB-1} + \rho_{PS} \times \omega_{PS}} \qquad (2)$$

Where ρ_{amorph}, $\rho_{crystal}$, and ρ_{PS} are the density of the PB-1's amorphous region(and melt), PB-1's crystalline region and PS(melt and solid state) respectively. X_c is the crystalline degree of PB-1 tubes (55%, calculated by DSC results) and ω_{PB-1}, ω_{PS} are the weight ratio of PB-1 and PS. In this study, ∇ is calculated to be 1.06. Tubes with different CFR were prepared to determine the optimal condition for the formation of PS microfibers. The common blend tubes were also prepared by taking the tubular extrudates off the die directly and cooled down by water spray. To manipulate the alignment of the in-situ formed PS microfibers, proper shear stress was imposed to the melt by the counter rotating mandrel and die. In this communication, the rotation rates of mandrel and die were both set at 4 rpm and the diameters of the produced microfibrillar tubes were 20mm to optimize the microfibrillation. The PS/PB-1 and pure PB-1 tubes prepared through rotation extrusion was denoted as RE-PSPB and RE-PB. And the PS/PB-1 and pure PB-1 tubes prepared through convention extrusion, during which the mandrel and die remain motionless, were denoted as CE-PSPB and CE-PB. All prepared samples were aged at room temperature for 10 days before testing, erasing the tetragonal form crystal.

Characterization

SEM: For Scanning Electronic Microscope observation, the samples were etched in a permanganic etchant[1] for 12h to partly remove the PB-1 matrix. Showing good resistance to permanganic etchant, the morphology of PS phase can be well exposed.[2] For the observation of cross-section, the samples were firstly cut by using a ultrathin slicer to generate a smooth cross-section plane before etching treatment(as shown in

Figure 2c.)

2D-SAXS and 2D-WAXD: Synchrotron two-dimensional small and wide angle X-ray scattering examinations were carried out in BL16B1 beamline in the Shanghai Synchrotron Radiation Facility (SSRF), Shanghai, China. The wavelength generated by the synchrotron radiation source was 0.124 nm and sample to detector distance was set at 100mm and 2200mm for 2D-WAXD and 2D-SAXS respectively (as shown in Figure 2d).

Mechanical performances tests: To examine the mechanical performances of the tubes, dog-bone shaped specimens were carefully cut from the produced tubes along the extrusion direction for ultimate axial strength (UAS) measurements; and the 50mm-long tubes were applied to tensile tress in the hoop direction until permanent damage had occurred to the tubes (yielding) and then the hoop damage strength (HDS) was calculated by the damage force(at yielding point) divided the product of tubes' average thickness(~1.6mm) and length(~50mm)(as shown in Figure 2a,b).

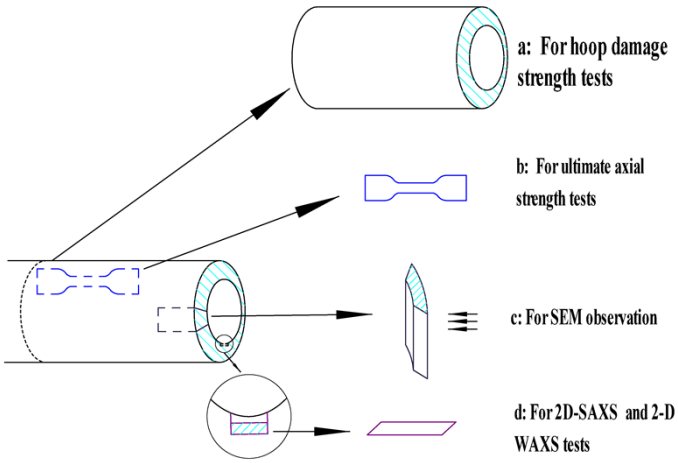

Figure 2. Illustration of characterization

Calculation of the length of PS "shish": The Ruland streak method[3] was applied to analyze the equatorial streak feature in 2D-SAXS. If one assume that the observed azimuthal distributions can be modeled by Lorentz functions, then the observed azimuthal width (B_{obs}), can be considered as a function of the length of shish($<L_{shish}>$) and the azimuthal width (B_ϕ) due to the misorientation of the shish, it follows as:

$$B_{obs} = \frac{2\pi}{< L_{shish} > q} + B_\phi$$

Here B_ϕ is the azimuthal width induced by the misorientation of the shish and B_{obs} represents the integral width of the azimuthal profile from the streak at a specific q, which is defied as the module of the scatter vector and can be calculated by: $q = 4\pi \sin\theta / \lambda$ (where the λ is the wavelength of the X-ray and 2θ is the scattering angle) [4].

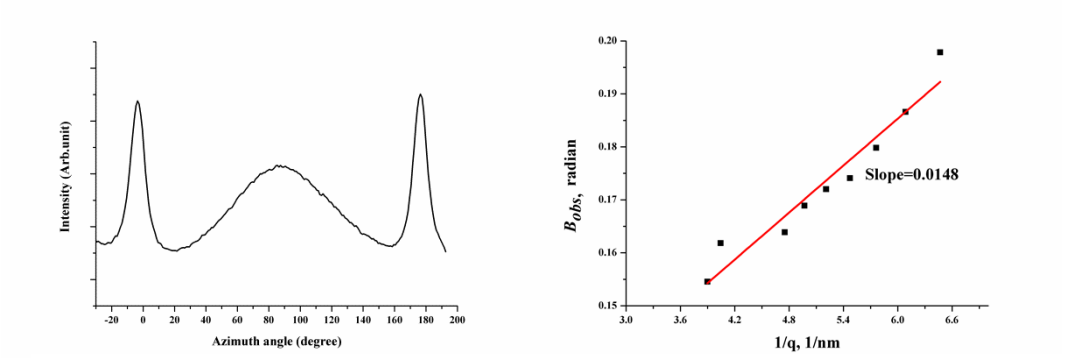

Figure 3. (a)The representative SAXS intensity distribution of equatorial streak along azimuthal angle, and (b) the plots of azimuthal width(B_{obs}) versus the value of 1/q

As can be seen from Figure 3b, the slope was calculated to be 0.0148. Then the length of the PS shish structure can be determined to be ~420nm.

References

1. A. Freedman, D. Bassett, A. Vaughan and R. Olley, *Polymer*, 1986, 27, 1163.

2. Z. Starý, T. Pemsel, J. Baldrian and H. Münstedt, *Polymer*, 2012, 53, 1881.

3. R. Perret and W. Ruland, *J Appl Crystallogr*, 1969, 2, 209.

4. K. Cui, L. Meng, N. Tian, W. Zhou, Y. Liu, Z. Wang, J. He and L. Li, *Macromolecules*, 2012, 45, 5477.